



Shahid Chamran
University of Ahvaz

Journal of Applied and Computational Mechanics



Research Paper

Stability Analysis of Mass Transfer on a Continuous Flat Plate Moving in Parallel or Reversely to a Free Stream in the Presence of Chemical Reaction by Haar Wavelets

Vishwanath B. Awati¹, N. Mahesh Kumar², Akash Goravar³

Department of Mathematics, Rani Channamma University, Belagavi, Karnataka-591156, India,
Email: awati.vb@rcub.ac.in (V.B.A.); maheshkumarmk98@gmail.com (N.M.K.); akash050992@gmail.com (A.G.)

Received December 27 2023; Revised May 09 2024; Accepted for publication June 16 2024.

Corresponding author: V.B. Awati (awati.vb@rcub.ac.in)

© 2024 Published by Shahid Chamran University of Ahvaz

Abstract. This study investigates two-dimensional viscous incompressible boundary layer flow involving mass transfer above an uninterrupted flat surface in the presence of chemical reaction. Applicable similarity transformations, transform the leading equations into a system of nonlinear ordinary differential equations. These equations are solved via collocation approach using Haar wavelets. The double solutions exist and are presented through graphs. The obtained solutions are confirmed by comparing them with earlier findings. The various physical quantities are enfolded and convinced carefully using numerical and theoretical approaches. Enhancement in Schmidt number increases the mass transfer rate for upper branch solution and reduces for lower branch solution. Mass immersion arises for constructive chemical reaction and mass transfer enhances for destructive chemical reaction. Finally, the stability analysis is performed.

Keywords: Boundary-layer flow; Chemical reaction; Haar wavelets; Dual solutions; Stability analysis.

1. Introduction

In a recent study, the boundary layer flow above a fixed flat plate is one of the conventional problems in fluid mechanics, and a literature review of boundary layer flow past a fixed plate through a uniform free stream is widely discussed. The laminar steady boundary layer flow above a fixed plate leads to a third-order nonlinear differential equation with infinite boundary by means of similarity variables was first studied by Blasius [1]. The Blasius problem is one of the simplest third-order nonlinear boundary value problem. Howarth [2] numerically determined the solution to various aspects of the Blasius problem. The boundary layer of an electrically conducting fluid flow over a vertical plate in the presence of an effective magnetic field that is regular to the flow was studied by Riley [3]. Abu-Sitta [4] discussed the existence of a solution of boundary layer flow past a fixed plate. The boundary layer flow over a fixed plate moving continuously along static velocity in an inactive fluid, and determined same problem as accomplished by Blasius for various boundary conditions was discussed by Sakiadis [5]. Abdulhafez [6] investigated the boundary layer problem for parallel stream over moving plate and resultant studies involve Blasius and Sakiadis problems as a special case. Afzal et al. [7] extended the model [6] by considering the momentum heat transfer. The effect of Hall on magnetohydrodynamics (MHD) past a continuously moving flat plate was deliberated by Watanabe and Pop [8]. The authors [9,10] prolonged the problems of Blasius and Sakiadis to examine the influence of thermal radiation. Hussaini et al. [11] analyzed the flow over a plane surface moving with static velocity in the opposing orientation of the stable mainstream. The aspects of mixed convection flow over moving in parallel or opposing to a free stream were discussed by Lin et al. [12]. The researchers [13-16] analyzed various aspects of the convective properties of fluid over different geometries under the influence of thermal radiation, heat transfer, and porous medium. Wang [17] determined an approximate solution of the Blasius equation using the A-domain decomposition method. The free convective unsteady flow of viscoelastic fluid above an infinite electrical conductivity of a vertical plate with an infinite insulator in the appearance of a transversal magnetic field was analyzed by Chowdhury [18]. In this area, many researchers [19-24] have conducted similar kinds of investigations for different conditions and obtained the important features of dual solutions.

The analysis of the boundary layer flow of a mass transfer produces the most important for the extension of the theory of divorce process and chemical kinetics. Also, the phenomenon of mass and heat transfer has accepted a significant consideration of contemporary investigators because of its immense pertinence in reservoir engineering, chemical industries, and numerous diverse processes. Chambre and Young [25] demonstrated the diffusion of a chemically reactive species in a laminar boundary layer flow over a flat surface. Soundalgekar [26] studied mass transfer gear as flow past an impetuously instituted vertical infinite



plate below many physical conditions. The investigators [27-29] analyzed the similarity solutions of the chemically reactive diffusion family for hybrid convection flow above a moving horizontal surface. The influence of chemical reaction and magnetic field for heat and mass transfer on laminar boundary layer flow across a semi-infinite horizontal plate was demonstrated by Anjalidevi and Kandasamy [30, 31]. Postelnicu [32] studied the Soret and Dufour impact for mass and heat transfer through free convection past a vertical surface in the presence of chemical reaction and permeable porous media. Bhattacharyya and Layek [33] determined the exhaustive similarity solutions of MHD enforced convective mass dissipation due to chemical reaction above a permeable porous surface through suction or blowing. Many researchers [34-39] analyzed the impact of chemical reaction on the stretching /shrinking sheet flow problems. Sachdev et al. [40] discussed the class of boundary value problems over unbounded domain by using semi-numerical methods. Kudenatti et al. [41] analyzed the solution to the problem of stretching plate through pressure gradient and suction by using an exact analytical method. Rasheed and Anwar [42] investigated the MHD flow of viscoelastic fluid and explored several important aspects of revised forms of thermal flux. Awati [43] and Makinde et al. [44] determined the Dirichlet series and approximate analytical methods for the solution of MHD boundary layer flow of Casson fluid over a stretching/ shrinking sheet problem. Awati et al. [45] examined the MHD flow problem with a linear stretching surface through approximate analytical method and Dirichlet series. The influence of an inclined magnetic field on the Ree-Eyring nanofluid model over a stretching surface was demonstrated through the differential transformation method by Puneeth et al. [46]. Awati [47] discussed an approximate analytical and Dirichlet series solution of MHD viscous flow due to a shrinking sheet as well as suction/blowing problems. Based on temperature-dependent properties, Alzahrani et al. [48] examined the micropolar fluid flow over a vertical stretching sheet. Hussian et al. [49] illustrated the significant impact of chemical reaction on hybrid nanofluid flow generated by curved nonlinear stretchable surface. Recently, Anwar et al. [50] addressed the fluid flow model in the presence of linear order chemical reaction with thermal radiation through finite difference and finite element approach.

Haar wavelet collocation method (HWCM) is one of the effective semi-numerical techniques for determining the solution of infinite boundary value problems (BVPs). The construction of HWCM involves a couple of piecewise constant approximation functions and these functions are integrated very easily. The important features of Haar approximations which are orthogonal and also form a reliable transform basis, the other properties are non-differentiable on account of disconnected in disintegrating points. In view of Lepik [51], there are two main properties to prevail over the difficulties. The first aspect is that the quadratic waves are normalized with interpolating splines etc. Chen and Hasio [52, 53] predicted the second one; for considering the derivative of the highest order involved in the equation can be expressed in terms of Haar functions. Lepik [54, 55] used the HWCM method to determine the solution of BVPs that automatically satisfy the boundary conditions. Majak et al. [56] studied the convergence of HWCM and predicted that the convergence is of order $O(1/2^{j-1})^2$, where J is the resolution level. Recently, Awati et al. [57] analyzed heat and mass transfer features during the convective boundary layer flow of a nanofluid moving over a nonlinearly stretching sheet through a Haar wavelet. Awati and Mahesh [58] discussed unnatural convection heat transfer over a stationary and moving semi-infinite plane with nanofluids using Haar wavelets. The choice of the HWCM is highly encouraged as it is easy to implement with less computation cost, utilizing a few numbers of grid points great amount of accuracy in the solution can be achieved in comparison with other available semi-numerical approaches. Finally, the method is extremely suitable for solving the boundary value problem as the boundary constraints are satisfied automatically.

From increasing computational/technological applications, innovative numerical and semi-numerical algorithms it is motivated to analyze the mass transfer under the influence of chemical reaction of first order on an uninterrupted moving horizontal plate with constant velocity in similar or reversely to a uniform free stream. Using the appropriate transformation variables, self-similar nonlinear ordinary differential equations (NLODEs) with infinite domain are derived from governing equations. These resultant equations are solved through a semi-numerical approach using HWCM. The impact of several parameters characterizing the governing flow is discussed in detail.

2. Mathematical Formulation

In the existence of linear order chemical reaction, consider viscous incompressible steady 2D laminar flow with mass transfer above the moving flat plate. Assume that the plate is advancing with fixed velocity U_w in a direction assisting or opposing to the flow and U_∞ be the velocity of a homogeneous free stream. The x -axis and y -axis are respectively assigned along the direction of the plate and normal to it, as shown in Fig. 1.

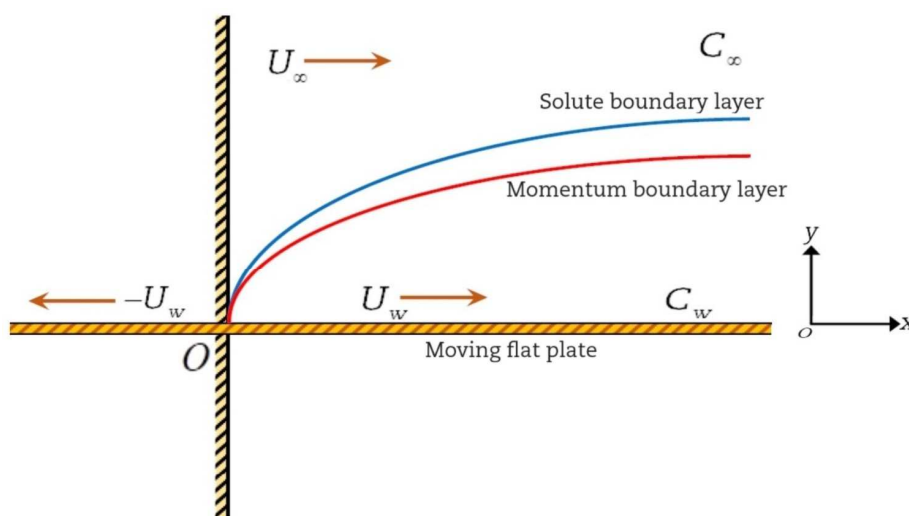


Fig. 1. The schematic diagram of the physical problem.



The governing equations of the flow based on boundary layer approximation and concentration distribution can be written as [39]:

$$\frac{\partial u}{\partial x} + \frac{\partial v}{\partial y} = 0, \quad (1)$$

$$u \frac{\partial u}{\partial x} + v \frac{\partial u}{\partial y} = \nu \frac{\partial^2 u}{\partial y^2}, \quad (2)$$

$$u \frac{\partial C}{\partial x} + v \frac{\partial C}{\partial y} = D \frac{\partial^2 C}{\partial y^2} - R(C - C_\infty), \quad (3)$$

where u and v are the components of velocities in x and y directions, respectively, $\nu (= \mu/\rho)$, μ , ρ , C , C_w , C_∞ , D and $R(x) = LR_0/x$ respectively denotes the kinematic viscosity, coefficient of fluid viscosity, density of the fluid, concentration, plate concentration, concentration at free stream, diffusion coefficient and variable reaction rate for constant R_0 and reference length L . The boundary constraints concerning velocity and concentrations for Eqs. (2) and (3) are:

$$u = U_w, \quad v = 0, \quad C = C_w \quad \text{at} \quad y = 0, \quad (4)$$

$$u \rightarrow U_\infty, \quad C \rightarrow C_\infty \quad \text{as} \quad y \rightarrow \infty, \quad (5)$$

The stream function $\psi(x,y)$ is expressed as:

$$u = \frac{\partial \psi}{\partial y} \quad \text{and} \quad v = -\frac{\partial \psi}{\partial x}. \quad (6)$$

Equation (1) satisfied directly in concerned with Eq. (6). Introducing the similarity variables for ψ and C as:

$$\eta = y \sqrt{\frac{U}{x\nu}}, \quad \psi = \sqrt{U\nu x} f(\eta) \quad \text{and} \quad C = C_\infty + (C_w - C_\infty) \phi(\eta), \quad (7)$$

where η represents similarity variable and $U = U_\infty + U_w$ is composite velocity [8]. Utilizing Eqs. (6) and (7) in Eqs. (2) and (3), the resultant equations become:

$$f''' + \frac{1}{2} f f'' = 0, \quad (8)$$

$$\phi'' + \frac{1}{2} Sc f \phi' - Sc \beta \phi = 0, \quad (9)$$

where $Sc = \nu/D$ and $\beta = LR_0/U$ are Schmidt number and reaction rate factor, respectively. The chemical reaction is destructive if $\beta > 0$ and constructive if $\beta < 0$.

The corresponding boundary constraints from Eqs. (4) and (5) are:

$$f(\eta) = 0, \quad f'(\eta) = \alpha, \quad \phi(\eta) = 1 \quad \text{at} \quad \eta = 0, \quad (10)$$

$$f'(\eta) \rightarrow 1 - \alpha, \quad \phi(\eta) \rightarrow 0 \quad \text{as} \quad \eta \rightarrow \infty, \quad (11)$$

where $\alpha = U_w U^{-1}$ is the ratio of velocity factor.

3. Haar Wavelets

The simplest orthonormal wavelet is a Haar wavelet with compact support and made up of piecewise constant functions. The features of these wavelets are explicitly expressed involving both scaling and wavelet functions, generating Haar matrices that are compactly supported, orthogonal, and sparse.

The domain of integration $\eta \in [P, Q]$ is divided into $2M$ equal subintervals of length $\delta\eta = (Q - P)/2M$, where $M = 2^j$, j designates the maximal level of resolution. The s^{th} Haar wavelet is defined as:

$$h_s(\eta) = \begin{cases} 1, & \text{for } \eta \in [\zeta_1(s), \zeta_2(s)), \\ -1, & \text{for } \eta \in [\zeta_2(s), \zeta_3(s)), \\ 0, & \text{elsewhere.} \end{cases} \quad (12)$$

where $\zeta_1(s) = P + 2k\mu\delta\eta$, $\zeta_2(s) = P + (2k + 1)\mu\delta\eta$, $\zeta_3(s) = P + 2(k + 1)\mu\delta\eta$, $\mu = M/m$,

$$s = m + k + 1, \quad m = 2^j. \quad (13)$$

For Eqs. (12) and (13), $j = 0, 1, 2, \dots, J$ and $k = 0, 1, 2, \dots, m - 1$ denotes the dilation and translation factors, respectively. For $s = 1$, the scaling Haar wavelet function becomes:

$$h_1(\eta) = \begin{cases} 1, & \eta \in [P, Q), \\ 0, & \text{elsewhere.} \end{cases}$$



The Haar wavelet expansion of $\hat{f}(x)$ over a finite interval $[P, Q]$ is expressed as:

$$\hat{f}(x) = \sum_{s=1}^{\infty} \tilde{a}_s h_s(x), \tag{14}$$

where \tilde{a}_s are the Haar wavelet coefficients as:

$$\tilde{a}_s = 2^j \int_P^Q \hat{f}(x) h_s(x) dx, \quad s = 1, 2, \dots, 2^j + k + 1. \tag{15}$$

To obtain the Haar wavelet coefficients through integral square error minimization condition, we have:

$$\int_P^Q E_M^2 dx \rightarrow 0, \quad |E_M| = |\hat{f}(x) - \hat{f}_M(x)|, \quad \hat{f}_M(x) = \sum_{s=0}^{2M} \tilde{a}_s h_s(x), \tag{16}$$

where $\hat{f}(x)$ and $\hat{f}_M(x)$ are respectively denotes the exact and approximate functions. The n^{th} order multiple-integral of Haar function of Eq. (12) is calculated as:

$$p_{n,s} = \underbrace{\int_P^{\eta} \int_P^{\eta} \dots \int_P^{\eta}}_{n \text{ - times}} h_s(x) dx^n = \frac{1}{(n-1)!} \int_P^{\eta} (t-x)^{n-1} h_s(x) dx,$$

where $1 \leq n \leq N$, $1 \leq s \leq 2M$. For $n=0$ tends to $h_s(\eta)$ and the integrals can be evaluated for other non-zero values as:

$$p_{n,s}(\eta) = \begin{cases} 0, & \text{for } \eta \in [P, \zeta_1(s)), \\ \frac{1}{n!} [\eta - \zeta_1(s)]^n, & \text{for } \eta \in [\zeta_1(s), \zeta_2(s)), \\ \frac{1}{n!} \{ [\eta - \zeta_1(s)]^n - 2[\eta - \zeta_2(s)]^n \}, & \text{for } \eta \in [\zeta_2(s), \zeta_3(s)), \\ \frac{1}{n!} \{ [\eta - \zeta_1(s)]^n - 2[\eta - \zeta_2(s)]^n + [\eta - \zeta_3(s)]^n \}, & \text{for } \eta \in [\zeta_3(s), Q). \end{cases} \tag{17}$$

This relation is valid for $s > 1$ and in the case of $s = 1$, we have $\zeta_1 = P$, $\zeta_2 = \zeta_3 = Q$ and:

$$p_{n,1}(\eta) = \frac{1}{n!} (\eta - P)^n. \tag{18}$$

For $1 \leq l \leq 2M$, consider the collocation points $\eta_l = 0.5(\bar{\eta}_l + \bar{\eta}_{l-1})$, where $\bar{\eta}_l$ designates the l^{th} lattice point with $\bar{\eta}_1 = P + l\delta\eta$, $1 \leq l \leq 2M$.

4. Solution Method by HWCM

Chen and Hasio's [52] procedure is employed to obtain the solution of the present problem. The higher order derivatives of Eqs. (8) and (9) are represented by means of Haar wavelet approximation as:

$$f'''(\eta) = \sum_{s=1}^{2M} \tilde{a}_s h_s(\eta) \quad \text{and} \quad \phi''(\eta) = \sum_{s=1}^{2M} \tilde{b}_s h_s(\eta), \tag{19}$$

where \tilde{a}_s, \tilde{b}_s are the unknown coefficients need to be determined. Using Eqs. (10) and (11), the corresponding lower-order derivatives of Eq. (19) can be written as:

$$f''(\eta) = f''(0) + \sum_{s=1}^{2M} \tilde{a}_s p_{1,s}(\eta), \tag{20}$$

$$f'(\eta) = \alpha + \eta f''(0) + \sum_{s=1}^{2M} \tilde{a}_s p_{2,s}(\eta) \quad \text{and} \quad \phi'(\eta) = \phi'(0) + \sum_{s=1}^{2M} \tilde{b}_s p_{1,s}(\eta), \tag{21}$$

$$f(\eta) = \alpha\eta + \frac{\eta^2}{2} f''(0) + \sum_{s=1}^{2M} \tilde{a}_s p_{3,s}(\eta) \quad \text{and} \quad \phi(\eta) = 1 - \eta\phi'(0) + \sum_{s=1}^{2M} \tilde{b}_s p_{2,s}(\eta). \tag{22}$$

Setting $\eta_{\infty} = Q$ and utilizing the boundary conditions, we have:

$$f''(0) = \frac{1}{Q} \left[1 - 2\alpha - \sum_{s=1}^{2M} \tilde{a}_s C_s^1 \right] \quad \text{and} \quad \phi'(0) = \frac{-1}{Q} \left[1 + \sum_{s=1}^{2M} \tilde{b}_s C_s^1 \right], \tag{23}$$

where $C_s^1 = \int_P^Q p_{1,s}(t) dt$. Substituting Eqs. (19)-(23) into Eqs. (8)-(9), we have:

$$\sum_{s=1}^{2M} \tilde{a}_s h_s(\eta) + \frac{1}{2} \left\{ \left[\alpha\eta + \frac{\eta^2}{2} \left(\frac{1}{Q} \left[1 - 2\alpha - \sum_{s=1}^{2M} \tilde{a}_s C_s^1 \right] \right) + \sum_{s=1}^{2M} \tilde{a}_s p_{3,s}(\eta) \right] \right\} \left\{ \frac{1}{Q} \left[1 - 2\alpha - \sum_{s=1}^{2M} \tilde{a}_s C_s^1 \right] + \sum_{s=1}^{2M} \tilde{a}_s p_{1,s}(\eta) \right\} = 0, \tag{24}$$



$$\sum_{s=1}^{2M} b_s h_s(\eta_h) + \left[\frac{1}{2} Scf(\eta) \left[\frac{-1}{Q} \left[1 + \sum_{s=1}^{2M} \tilde{b}_s C_s^1 \right] + \sum_{s=1}^{2M} \tilde{b}_s p_{1,s}(\eta_h) \right] - \left[Sc\beta \left[1 - \eta \left[\frac{-1}{Q} \left[1 + \sum_{i=1}^{2M} \tilde{b}_s C_s^1 \right] \right] + \sum_{i=1}^{2M} \tilde{b}_s p_{2,s}(\eta_h) \right] \right] \right] = 0, \tag{25}$$

where $h_s(\eta_h)$, $p_{1,s}(\eta_h)$, $p_{2,s}(\eta_h)$ and $p_{3,s}(\eta_h)$ are square matrices of order $2^{J+1} \times 2^{J+1}$ and C_s^1 is column matrix of corresponding order for $l=1, 2, 3, \dots, 2^{J+1}$. The advantage of this procedure is to reduce the calculation period and rapid implementation for the solution of boundary value problems. The coefficients \tilde{a}_s and \tilde{b}_s are determined by using Netown's method. The technique involves the selection of non-trivial two collocation points at $J=0$. Obtained approximations are utilized for proceeding resolution levels sequentially. The process is carried out until the desired accuracy in the results is reached and these results are presented through tables and graphs.

4.1. Error estimation

The effectiveness of HWCMM is verified by assessing the errors in the calculated numerical results.

- a. For the known exact solution cases the L_∞ errors are expressed as $E_f(J) = \max_{1 \leq l \leq 2^{J+1}} |f(\eta_h)^{exact} - f(\eta_h)^{num}|$ and $E_\phi(J) = \max_{1 \leq l \leq 2^{J+1}} |\phi(\eta_h)^{exact} - \phi(\eta_h)^{num}|$.
- b. For the unknown analytical solution cases the degree exactness of Haar wavelet approximations is evaluated through solution error, given by the relation:

$$\sigma_f(J) = \|\Delta_f^f(\eta_h)\| / 2^{J+1} \text{ and } \sigma_\phi(J) = \|\Delta_\phi^\phi(\eta_h)\| / 2^{J+1} \tag{26}$$

where $\Delta_f^f(\eta_h) = f_j(\eta_h) - f_{j+1}(\eta_h)$, $\Delta_\phi^\phi(\eta_h) = \phi_j(\eta_h) - \phi_{j+1}(\eta_h)$, $\{f_j(\eta_h), \phi_j(\eta_h)\}$ and $\{f_{j+1}(\eta_h), \phi_{j+1}(\eta_h)\}$ are the solutions obtained at the resolution level J and $J+1$, respectively.

In the present Haar wavelets calculation, it is observed that there is an inverse relationship between the error and J . The obtained results concerning error for various resolution levels are depicted in Fig. 2.

5. Stability Analysis

For stability analysis, according to the Merkin [59] and Weidman et al. [21], the unsteady form of the problem is considered. The continuity Eq. (1) holds, whereas Eq. (2) and Eq. (3) are written as:

$$\frac{\partial u}{\partial t} + u \frac{\partial u}{\partial x} + v \frac{\partial u}{\partial y} = v \frac{\partial^2 u}{\partial y^2}, \tag{27}$$

$$\frac{\partial C}{\partial t} + u \frac{\partial C}{\partial x} + v \frac{\partial C}{\partial y} = D \frac{\partial^2 C}{\partial y^2} - R(C - C_\infty), \tag{28}$$

where t represents the time. Introducing dimensionless variables as follows:

$$\psi = \sqrt{Uv\alpha} f(\eta, \tau), \quad \eta = y \sqrt{\frac{U}{\alpha x}}, \quad \phi(\eta, \tau) = \frac{C - C_\infty}{C_w - C_\infty} \quad \text{and} \quad \tau = \frac{Ut}{\alpha} \tag{29}$$

The transformed versions of Eq. (27) and (28) can be expressed as:

$$\frac{\partial^3 f}{\partial \eta^3} + \frac{1}{2} f \frac{\partial^2 f}{\partial \eta^2} - \frac{\partial^2 f}{\partial \eta \partial \tau} = \tau \left[\frac{1}{2} \frac{\partial f}{\partial \tau} \frac{\partial^2 f}{\partial \eta^2} - \frac{\partial f}{\partial \eta} \frac{\partial^2 f}{\partial \eta \partial \tau} \right], \tag{30}$$

$$\frac{\partial^2 \phi}{\partial \eta^2} + \frac{Sc}{2} f \frac{\partial \phi}{\partial \eta} - Sc\beta\phi - Sc \frac{\partial \phi}{\partial \tau} = Sc\tau \left[\frac{1}{2} \frac{\partial f}{\partial \tau} \frac{\partial \phi}{\partial \eta} - \frac{\partial f}{\partial \eta} \frac{\partial \phi}{\partial \tau} \right], \tag{31}$$

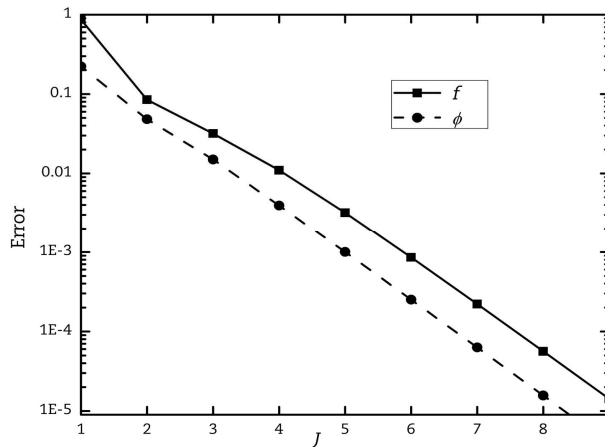


Fig. 2. Error vs. resolution level J for $Sc = 0.5$, $\beta = 0$ and $\alpha = 1$.



The relevant boundary conditions are:

$$f(0, \tau) = \tau f_\tau(0, \tau), \quad \frac{\partial f}{\partial \eta}(0, \tau) = \alpha, \quad \phi(0, \tau) = 0 \quad \text{at} \quad \eta = 0, \tag{32}$$

$$\frac{\partial f}{\partial \eta}(\eta, \tau) \rightarrow 1 - \alpha, \quad \phi(\eta, \tau) \rightarrow 0 \quad \text{as} \quad \eta \rightarrow \infty. \tag{33}$$

To examine the stability of steady flow, $f(\eta) = f_0(\eta)$ and $\phi(\eta) = \phi_0(\eta)$ satisfy the boundary-value problem (30)-(33), adapting the technique of Weidman et al. [21] by putting:

$$f(\eta, \tau) = f_0(\eta) + e^{-\lambda\tau} F(\eta, \tau), \tag{34}$$

$$\phi(\eta, \tau) = \phi_0(\eta) + e^{-\lambda\tau} G(\eta, \tau), \tag{35}$$

where $F(\eta, \tau)$ and $G(\eta, \tau)$ are small relative to $f_0(\eta)$ and $\phi_0(\eta)$, respectively, and λ is an eigenvalue to be determined. Infinite eigenvalues $\lambda_1 < \lambda_2 < \lambda_3 < \dots$ are obtained from the solution of the eigenvalue problem (30)-(33), if the smallest eigenvalue is less than zero, there is an initial growth of disturbance and unstable flow occurs. Whereas, the flow becomes stable for the smallest positive eigenvalue due to the initial decay of disturbance.

Using Eqs. (34) and (35) into Eqs. (30) and (31), and linearization gives:

$$\frac{\partial^3 F}{\partial \eta^3} + \frac{1}{2} f_0 \frac{\partial^2 F}{\partial \eta^2} + \frac{1}{2} f_0'' F + \lambda \frac{\partial F}{\partial \eta} - \frac{\partial^2 F}{\partial \eta \partial \tau} = \tau \left[\frac{1}{2} f_0'' \left(\frac{\partial F}{\partial \tau} - \lambda F \right) - f_0' \left(\frac{\partial^2 F}{\partial \eta \partial \tau} - \lambda \frac{\partial F}{\partial \eta} \right) \right], \tag{36}$$

$$\frac{\partial^2 G}{\partial \eta^2} + \frac{Sc}{2} f_0 \frac{\partial G}{\partial \eta} + \frac{Sc}{2} \phi_0' F - (\beta - \lambda) Sc G - Sc \frac{\partial G}{\partial \tau} = Sc \tau \left[\frac{1}{2} \phi_0' \left(\frac{\partial F}{\partial \tau} - \lambda F \right) - f_0' \left(\frac{\partial G}{\partial \tau} - \lambda G \right) \right], \tag{37}$$

The resultant boundary conditions are:

$$F(0, \tau) = \frac{\tau}{e^{-\lambda\tau}} f_\tau(0, \tau), \quad \frac{\partial F}{\partial \eta}(0, \tau) = 0, \quad G(0, \tau) = 0 \quad \text{at} \quad \eta = 0, \tag{38}$$

$$\frac{\partial F}{\partial \eta}(\eta, \tau) \rightarrow 0, \quad G(\eta, \tau) \rightarrow 0 \quad \text{as} \quad \eta \rightarrow \infty. \tag{39}$$

The steady-state solutions $f(\eta) = f_0(\eta)$ and $\phi(\eta) = \phi_0(\eta)$ of Eqs. (36) and (37) are achieved by setting $\tau = 0$. The functions $F(\eta) = F_0(\eta)$ and $G(\eta) = G_0(\eta)$ in Eqs. (36) and (37) investigate the initial growth or decay of Eqs. (34) and (35). For this, the following linear eigenvalue problem needs to be solved:

$$F_0''' + \frac{1}{2} f_0 F_0'' + \frac{1}{2} f_0'' F_0 + \lambda F_0' = 0, \tag{40}$$

$$G_0'' + \frac{Sc}{2} f_0 G_0' + \frac{Sc}{2} \phi_0' F_0 - (\beta - \lambda) Sc G_0 = 0, \tag{41}$$

The corresponding boundary conditions are:

$$F_0(\eta) = 0, \quad F_0'(\eta) = 0, \quad G_0(\eta) = 0 \quad \text{at} \quad \eta = 0, \tag{42}$$

$$F_0'(\eta) \rightarrow 0, \quad G_0(\eta) \rightarrow 0 \quad \text{as} \quad \eta \rightarrow \infty. \tag{43}$$

The stability of solution of a steady-state flow is done by determining the smallest eigenvalue λ_1 , which follows from Harris et al. [60], the condition $F_0'(\eta) \rightarrow 0$ as $\eta \rightarrow \infty$ has been rested and solving Eqs. (40) and (41) numerically for a fixed value of λ satisfying the boundary condition (42).

Table 1. The numerical values of $f''(0)$ for α various values.

α	Blasius [1]	Sakiadis [5]	Ishak et al. [20]		Bhattacharyya [39]		HWCM	
			Upper branch	Lower branch	Upper branch	Lower branch	Upper branch	Lower branch
-0.5	---	---	0.3990	0.1710	0.39895	0.17103	0.397861	0.171025
-0.4	---	---	0.4357	0.0834	0.43566	0.08336	0.435601	0.083230
-0.3	---	---	0.4339	0.0367	0.43387	0.03672	0.433867	0.033470
-0.2	---	---	0.4124	0.0114	0.412437	0.01143	0.412369	0.0114
-0.1	---	---	0.3774	0.0010	0.37739	0.00105	0.377389	0.0010
0	0.332	---	0.3321	---	0.33206	---	0.332060	---
0.5	---	---	0	---	0	---	0	---
1	---	-0.4438	-0.4438	---	-0.44375	---	-0.443923	---



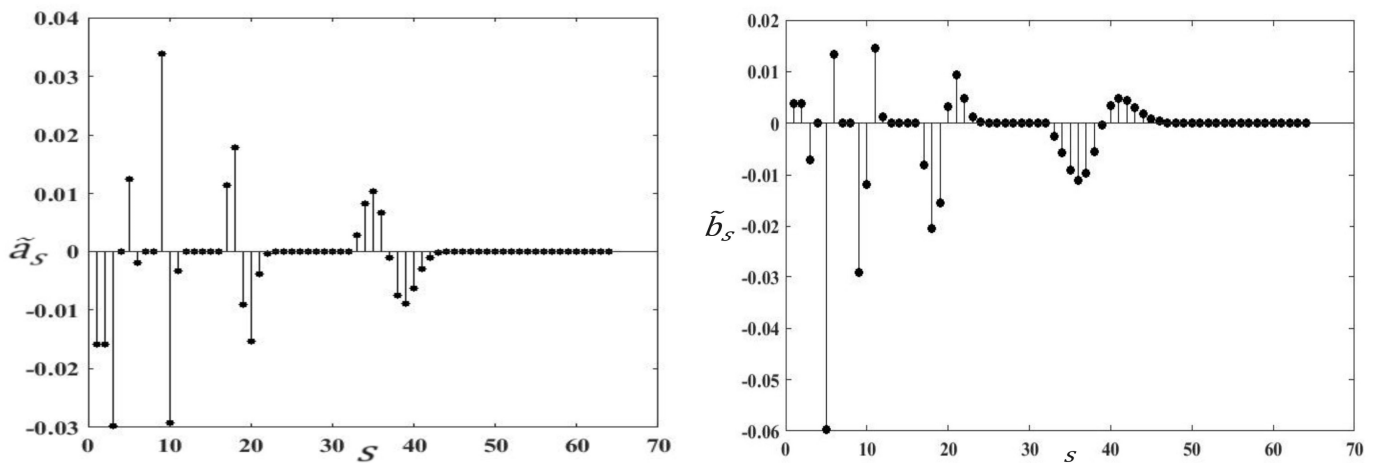
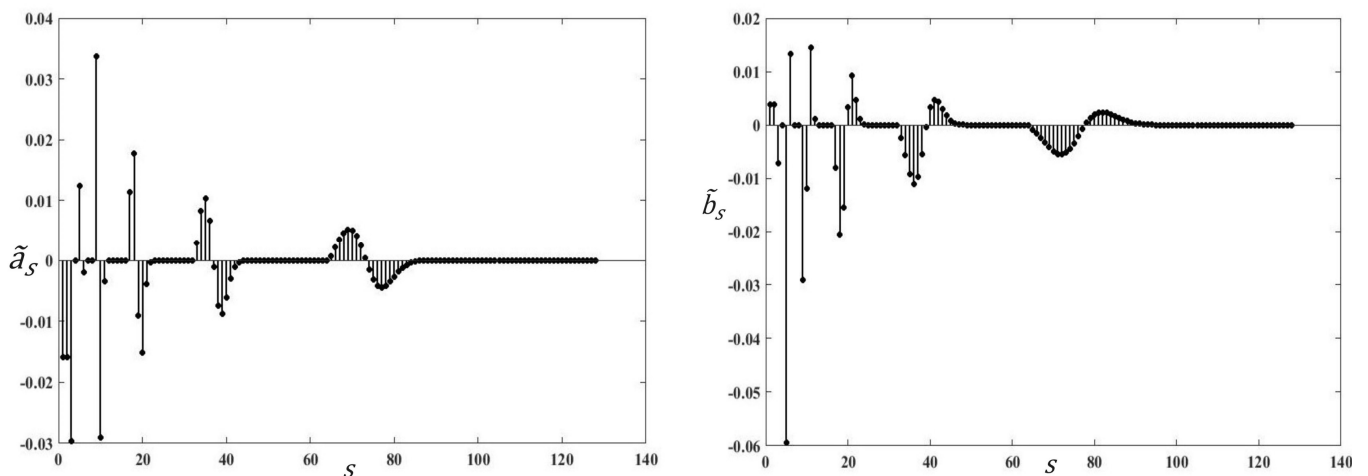
Table 2. The smallest eigenvalue λ_1 for various values of α .

α	Upper branch	Lower branch
-0.2	0.32050	-0.07728
-0.3	0.26622	-0.09541
-0.4	0.19913	-0.09821
-0.5	0.10585	-0.07325
-0.51	0.09305	-0.06723
-0.54	0.04050	-0.03499
-0.548	0.00676	-0.00647
-0.548247	0.00002	-0.00001

6. Result and Discussion

The semi-numerical method described in section 4 is used to determine the solution of self-similar Eqs. (8) and (9), satisfying the boundary constraints (10) and (11) for various values of governing parameters viz. the Schmidt number (Sc), velocity ratio parameter (α), and reaction ratio parameter (β). The influence of these parameters on the solutions is studied and obtained outcomes are expressed through tables and graphs. The skin friction coefficients, $f''(0)$, for different values of α are obtained using HWCM agree with a solution by Blasius [1], Sakiadis [5], Ishak et al. [20], and Bhattacharyya [39] as presented in Table 1.

Figure 2 shows the estimation of error along the resolution level, initially the error is too high and later it reduces as the resolution level increases. The maximum error is drawn and error estimation is determined at each point of the domain of the flow. To estimate error $\sigma(J)$ given in Eq. (26) is analyzed before finding the solution. In the present case, the coupled nonlinear system of Eqs. (8) and (9) obeying the boundary constraints (10) and (11) which cannot be solved in terms of closed form. The variations in the solution error $\sigma(J)$ for $\alpha = 1$, $\beta = 0$ and $Sc = 0.5$ is predicted by Eq. (26) and are shown in Fig. 2. It depicts that enhancement in J reduces the error curve for f and ϕ on log scale and causes degrading of error to the tolerance. Also, the error decreases much faster which shows the efficiency of HWCM.

Fig. 3. Haar wavelet coefficients \tilde{a}_s and \tilde{b}_s for resolution $J = 5$ at $\alpha = 0$, $\beta = 0.2$ and $Sc = 1$.Fig. 4. Haar wavelet coefficients \tilde{a}_s and \tilde{b}_s for resolution $J = 6$ at $\alpha = 0$, $\beta = 0.2$ and $Sc = 1$.

In this semi-numerical method, we shall discuss two important aspects in detail. The first case, determination of unknown Haar coefficients \tilde{a}_s and \tilde{b}_s to obtain the convergent solution of the flow problem, which does not depend upon the flow parameters but varies with the resolution level J . As J increases, i.e., $J = 5$ or 6 , the number of coefficients \tilde{a}_s and \tilde{b}_s in the series of Eq. (23) also increases by 64 or 128 coefficients. Figures 3 and 4 present the coefficients of \tilde{a}_s and \tilde{b}_s for $\alpha = 1$, $\beta = 0.2$ and $Sc = 1$, depicts the value of the coefficient approaches to zero. Also, using a few number terms in the series produces a more accurate solution. In the second case, the coefficients \tilde{a}_s and \tilde{b}_s are either positive or negative and follow the same pattern for different resolution levels, these coefficients are small in the sense of absolute value. The sign changes in the coefficients indicate that the solution experiences the breakdown.

The four different cases of α have been studied; the first one, $0 < \alpha < 1$, the fluid and plate move in the parallel long same orientation, the second situation deals with an immovable plate for $\alpha = 0$; the third circumstance is $\alpha < 0$ or $\alpha > 1$, for the fluid and plate moving in the opposite direction and the last case, $\alpha = 1$, for the movement of the plate in absence of fluid velocity [5]. In this study, the value of $\alpha \leq 1$ is considered. In literature [7, 20] similar kind of discussion is made and observed that the solution obtained is unique when $\alpha > 0$, dual natured solution exists when $-0.548427 \leq \alpha \leq 0$ and no boundary layer exists when $\alpha < -0.548427$, i.e. separation occurrence between plate surface and boundary layer. The variation of $f''(0)$ with α is demonstrated in Fig. 5 and the dual solutions are evaluated. The values of $f''(0)$ for lower branch reduce and for the upper branch, they initially increase (for some negative values of α and gradually decay with α).

Figures 6 and 7 present the values of concentration gradient at the plate $-\phi'(0)$, is proportional to the mass transfer rate against α for various values of Sc and β , respectively. The solution with a dual nature is encountered for concentration distributions. Further, the enhancement in Sc enhances the values of $-\phi'(0)$ for upper-branch solutions and drops in the case of lower-branch solutions. For both solutions, the values of $-\phi'(0)$ decreases and increases respectively for the constructive and destructive chemical reaction due to the mass transfer rate. For a constructive chemical reaction, it is observed that mass absorption takes place concerning certain values of α . Whereas, in the case of upper branch solution the absorption of mass for constructive reactions occurs when α approaches to unity and for lower branch solutions mass absorption rate is higher with an increase of α for constructive chemical reaction. Blasius [1] and Sakiadis [5] found that the upper branch solution which is only one solution in the range $0 \leq \alpha \leq 1$. The discussion made in section 5 and Table 2 reveals that the upper branch solutions are stable with positive eigenvalues and lower branch solutions are unstable with negative eigenvalues.

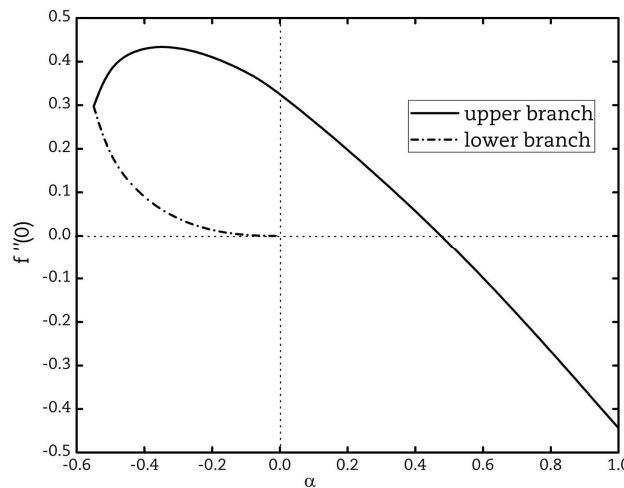


Fig. 5. Skin friction coefficient $f''(0)$ for various values of α at $Sc = 1$ and $\beta = 0$.

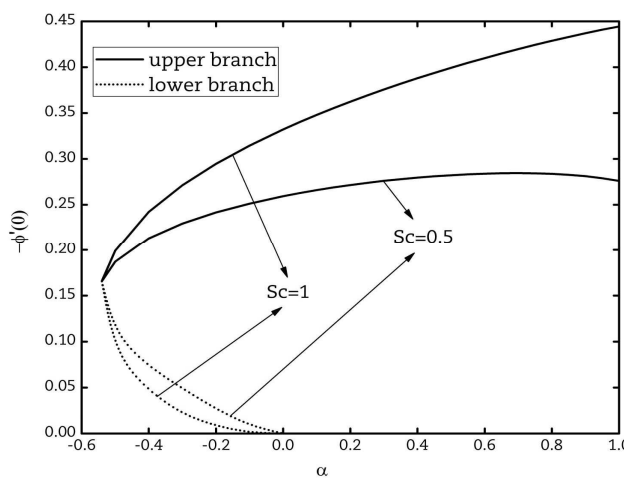


Fig. 6. Concentration gradient at the sheet $-\phi'(0)$ vs. α for various values Sc at $\beta = 0$.



Figures 8 and 9 present the variations in velocity $f'(\eta)$ and concentration $\phi(\eta)$ profiles respectively concerning with α , the dual profiles are drawn ($\alpha < 0$). It predicts that, with enhancement in magnitude of α , the thickness of the momentum boundary layer enhances for the upper branch and reduces for lower branch solutions as shown in Fig. 8. Concerning to the enhancement in the magnitude of α , $\phi(\eta)$ at a particular point strictly increases for upper branch and exhibits the reverse nature for the lower branch solutions. Also, the thickness of the solute boundary layer enhances and reduces respectively for upper and lower branch profiles with increasing values of α (in sense of magnitude). The graphs reveal that in comparison with the upper branch solution, the thickness of boundary layer flow for lower branch solutions is always thicker.

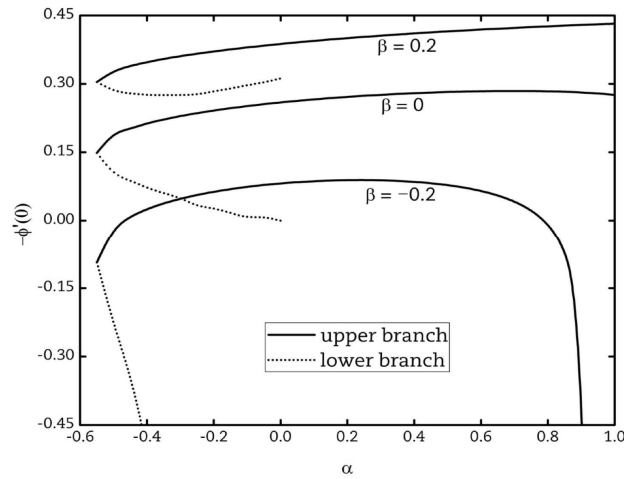


Fig. 7. Concentration gradient at the sheet $-\phi'(0)$ vs. α for various values of β at $Sc = 0.5$.

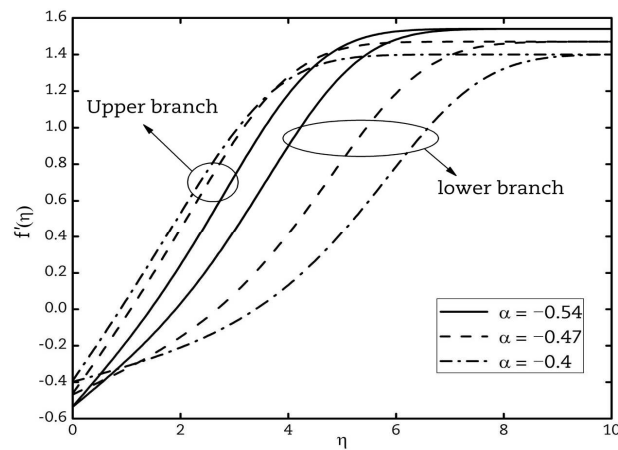


Fig. 8. Velocity profiles $f'(0)$ for various values of α .

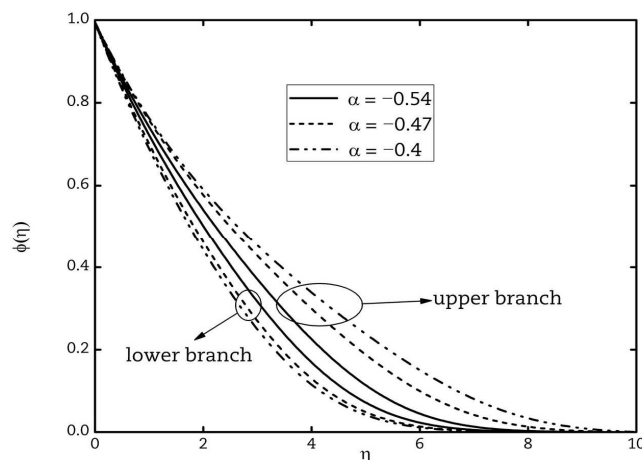


Fig. 9. Concentration profiles $\phi(\eta)$ for various values of α at $Sc = 0.5$ and $\beta = 0.2$.



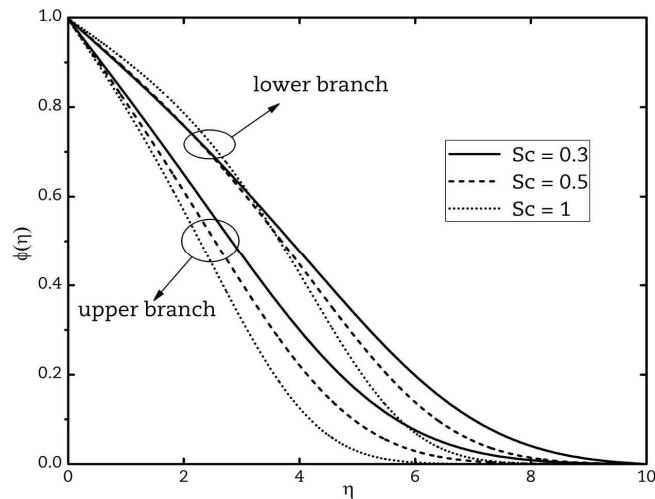


Fig. 10. Concentration profiles $\phi(\eta)$ for different values at $\alpha = -0.5$, $\beta = 0$.

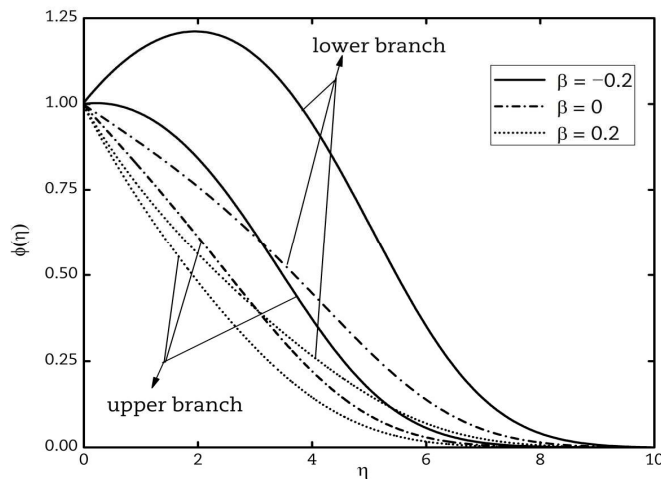


Fig. 11. Concentration of $\phi(\eta)$ for various values of β at $Sc = 0.5$ and $\alpha = -0.5$.

Figure 10 demonstrates the variations in profiles of $\phi(\eta)$ for different values of Sc . The dual nature concentration profiles exhibited that the lower branch profiles of the non-dimensional concentration $\phi(\eta)$ initially increases with increasing values Sc , get reverted in the mid-region, and curves tend to merge in the far field region. Whereas, the profiles of $\phi(\eta)$ show the contrary behavior of upper branch profiles concerning with increasing values of Sc at any point. The definition of Sc confirms the inverse relationship among the mass diffusivity and Sc . Thus, the concentration thicknesses of the boundary layer for both solutions decrease due to enhancement of Sc . In reality, the solute boundary layer thickness becomes thinner which causes a reduction in diffusion coefficient due to an increase in Sc .

In Fig. 11, the variation of concentration profiles for various values of β is illustrated. In destructive chemical reaction, the thickness of the solute boundary layer and solute profiles of both solutions decreases. In particular, for constructive chemical reaction both solution profiles increase. It is also significant to view that the appearance of concentration exceeds for the constructive reaction which indicates that the mass absorption occurs and it confirms that the negative value of $-\phi'(0)$ for $\beta < 0$ in some conditions. Physically, intensified constructive chemical reaction parameter leads to constructive chemical reaction of higher rate that efficiently produce a greater amount of fluid species and result in an increase of concentration distribution. For destructive chemical reaction factor the opposite trend is noticed as reported in [50].

7. Conclusion

Based on the above analysis, the following conclusions are drawn:

- a. The method discloses a double solution for the concentration distribution with a velocity field in the interval $-0.548427 \leq \alpha \leq 0$.
- b. The increase in Schmidt number leads to decreases in the thickness of the concentration boundary layer for upper and lower branch solutions.
- c. The stability analysis of the problem reveals, due to negative eigenvalues the lower branch solution is unstable, and the upper branch solution is stable as obtained in the case of eigenvalues are positive.



Author Contributions

V.B. Awati and N. Mahesh Kumar proposed and verified the problem. V.B. Awati and A. Goravar addressed the stability analysis for the problem. V.B. Awati supervised the entire work. The manuscript was written through the contribution of all authors. All authors discussed the results, reviewed, and approved the final version of the manuscript.

Acknowledgments

We are thankful to the anonymous reviewers for their valuable comments.

Conflict of Interest

The authors declared no potential conflicts of interest concerning the research, authorship, and publication of this article.

Funding

The authors received no financial support for the research, authorship, and publication of this article.

Data Availability Statements

The datasets generated and/or analyzed during the current study are available from the corresponding author on reasonable request.

Nomenclature

C	Concentration [kg/m^3]	R_0	Constant
C_w, C_∞	Plate and free stream concentrations [kg/m^3]	Sc	Schmidt number
D	Diffusion coefficient [m^2/s]	U	Composite velocity [m/s]
f	Non-dimensional stream function	U_w	Plate velocity [m/s]
f'	Dimensionless velocity	U_∞	Free stream velocity [m/s]
L	Reference length [m]	u, v	Velocity components [m/s]
R	Variable reaction rate [$1/\text{s}$]	x, y	Distance along the plate [m]

Greek symbols

α	Velocity ratio parameter	ρ	Fluid density [kg/m^3]
β	Reaction rate parameter	ν	Kinematic viscosity [m^2/s]
η	Similarity variable	ϕ	Non-dimensional concentration
μ	Coefficient of fluid viscosity [$\text{kg}/(\text{m}\cdot\text{s})$]	ψ	Stream function

References


- [1] Blasius, H., Grenzschichten in Flüssigkeiten mit kleiner Reibung, *Zeitschrift für Mathematik und Physik*, 56(1), 1908, 1-37.
- [2] Howarth, L., On the solutions of laminar boundary layer equations, *Proceedings of the Royal Society A, London*, 164(919), 1938.
- [3] Riely, N., Magnetohydrodynamics free convection, *Journal of Fluid Mechanics*, 18(4), 1964, 577-586.
- [4] Abu-Sitta, A.M.M., A note on a certain boundary-layer equation, *Applied Mathematics and Computation*, 64(1), 1994, 73-77.
- [5] Sakiadis, B.C., Boundary-layer behaviour on continuous solid surfaces: Boundary-layer equations for two dimensional and axisymmetric flow, *AIChE Journal*, 7(1), 1961, 26-28.
- [6] Abdulhafez, T.A., Skin friction and heat transfer on a continuous flat surface moving in a parallel free stream, *International Journal of Heat and Mass Transfer*, 28(6), 1985, 1234-1237.
- [7] Afzal, N., Badaruddin, A., Elgarvi, A., Momentum and heat transport on a continuous flat surface moving in a parallel stream, *International Journal of Heat and Mass Transfer*, 36(13), 1993, 3399-3403.
- [8] Watanabe, T., Pop, I., Hall effect on magneto-hydrodynamic boundary layer flow over a continuous moving flat plate, *Acta Mechanica*, 108(1), 1995, 35-47.
- [9] Bataller, R.C., Radiation effects in the Blasius flow, *Applied Mathematics and Computation*, 198(1), 2008, 333-338.
- [10] Cortell, R., Numerical solution of classical Blasius flat-plate problem, *Applied Mathematics and Computation*, 170(1), 2005, 706-710.
- [11] Hussaini, M.Y., Lakin, W.D., Nachman, A., On similarity solutions of a boundary layer problem with an upstream moving wall, *SIAM Journal of Applied Mathematics*, 47(4), 1987, 699-709.
- [12] Lin, H.T., Wu, K.Y., Hoh, H.L., Mixed convection from an isothermal horizontal plate moving in parallel or reversely to a free stream, *International Journal of Heat and Mass Transfer*, 36(14), 1993, 3547-3554.
- [13] Afzal, N., Hussain, T., Mixed convection over a horizontal plate, *Journal of Heat Transfer*, 106(1), 1984, 240-241.
- [14] Yao, L.S., Two-dimensional mixed convection along a flat plate, *Journal of Heat Transfer*, 109(2), 1987, 440-445.
- [15] Hsu, C.T., Cheng, T., The Brinkman model for natural convection about a semi-infinite vertical flat plate in a porous medium, *International Journal of Heat and Mass Transfer*, 28(3), 1985, 683-697.
- [16] Mukhopadhyay, S., Layek, G.C., Radiation effects on force convective flow and heat transfer over a porous plate in a porous medium, *Meccanica*, 44(5), 2009, 587-597.
- [17] Wang, L., A new algorithm for solving classical Blasius equation, *Applied Mathematics and Computation*, 157(1), 2004, 1-9.
- [18] Chowdhury, M.M.K., Effect of free convection flow of a visco-elastic fluid past an infinite vertical flat plate in presence of transverse magnetic field, *Chemical Engineering Research Bulletin*, 10, 2007, 11-31.
- [19] Ishak, A., Nazar, R., Pop, I., Boundary-layer flow of a micropolar fluid on a continuously moving or fixed permeable surface, *International Journal of Heat and Mass Transfer*, 50(23-24), 2007, 4743-4748.
- [20] Ishak, A., Nazar, R., Pop, I., Flow and heat transfer characteristics on a moving flat plate in a parallel stream with constant surface heat flux, *Heat and Mass Transfer*, 45(5), 2009, 563-567.
- [21] Weidman, P.D., Kubitschek, D.G., Davis, A.M.J., The effect of transpiration on self-similar boundary layer flow over moving surfaces, *International*





Journal of Engineering Science, 44(11-12), 2006, 730–737.

- [22] Wang, C.Y., Stagnation flow towards a shrinking sheet, *International Journal of Non-linear Mechanics*, 43(5), 2008, 377–382.
- [23] Ishak, A., Nazar, R., Pop, I., Dual solutions in mixed convection flow near a stagnation point on a vertical surface in a porous medium, *International Journal of Heat and Mass Transfer*, 51(5-6), 2008, 1150–1155.
- [24] Bachok, N., Ishak, A., Pop, I., Unsteady boundary-layer flow and heat transfer of a nanofluid over a permeable stretching/shrinking sheet, *International Journal of Heat and Mass Transfer*, 55(7-8), 2012, 2102–2109.
- [25] Chambre, P.L., Young, J.D., On diffusion of a chemically reactive species in a laminar boundary layer flow, *The Physics of Fluids*, 1(1), 1958, 48–54.
- [26] Soundalgekar, V.M., Effects of mass transfer and free convective currents on the flow past an impulsively started vertical plate, *ASME Journal of Applied Mechanics*, 46(4), 1979, 757–760.
- [27] Soundalgekar, V.M., Birajdar, N.S., Darvekar, V.K., Mass transfer Effects on the flow past an impulsively started infinite vertical plate with variable temperature or constant heat flux, *Astrophysics and Space Science*, 100(1), 1984, 159–164.
- [28] Das, U.N., Deka, R., Soundalgekar, V.M., Effect of mass transfer on flow past an impulsively started infinite vertical plate with constant heat flux and chemical reaction, *Forschung im Ingenieurwesen*, 60(10), 1994, 284–287.
- [29] Muthucumaraswamy, R., Ganesan, P., First order chemical reaction on the flow past an impulsively started vertical plate with uniform heat and mass flux, *Acta Mechanica*, 147(1), 2001, 45–57.
- [30] Anjalidavi, S.P., Kandasamy, R., Effect of chemical reaction, heat and mass transfer on laminar flow along a semi-infinite horizontal plate, *Heat and Mass Transfer*, 35(6), 1999, 465–467.
- [31] Anjalidavi, S.P., Kandasamy, R., Effects of chemical reaction, heat and mass transfer on MHD flow past a semi infinite plate, *Zeitschrift für Angewandte Mathematik und Mechanik*, 80(10), 2000, 697–700.
- [32] Postelnicu, A., Influence of chemical reaction on heat and mass transfer by natural convection from vertical surfaces in porous media considering Soret and Dufour effects, *Heat and Mass Transfer*, 43(6), 2007, 595–602.
- [33] Bhattacharyya, K., Layek, G.C., Similarity solution of MHD boundary layer flow with diffusion and chemical reaction over a porous flat plate with suction/blowing, *Meccanica*, 47(4), 2012, 1043–1048.
- [34] Anderson, H.I., Hansen, O.R., Holmedal, B., Diffusion of a chemically reactive species from a stretching sheet, *International Journal of Heat and Mass Transfer*, 37(4), 1994, 659–664.
- [35] Chamkha, A.J., Aly, A.M., Mansour, M.A., Similarity solution for unsteady heat and mass transfer from a stretching surface embedded in a porous medium with suction/injection and chemical reaction effects, *Chemical Engineering Communications*, 197(6), 2010, 846–858.
- [36] Kandasamy, R., Periasamy, K., Sivagnana Prabhu, K.K., Chemical reaction, heat and mass transfer on MHD flow over a vertical stretching surface with heat source and thermal stratification effects, *International Journal of Heat and Mass Transfer*, 48(21-22), 2005, 4557–4561.
- [37] Bhattacharyya, K., Layek, G.C., Chemically reactive solute distribution in MHD boundary layer flow over a permeable stretching sheet with suction or blowing, *Chemical Engineering Communications*, 197(12), 2010, 1527–1540.
- [38] Bhattacharyya, K., Layek, G.C., Slip effect on diffusion of chemically reactive species in boundary layer flow over a vertical stretching sheet with suction or blowing, *Chemical Engineering Communications*, 198(11), 2011, 1354–1365.
- [39] Bhattacharyya, K., Mass transfer on a continuous flat plate moving in parallel or reversely to a free stream in the presence of a chemical reaction, *International Journal of Heat and Mass Transfer*, 55(13-14), 2012, 3482–3487.
- [40] Sachdev, P.L., Bujurke, N.M., Awati, V.B., Boundary Value Problems for Third-Order Nonlinear Ordinary Differential Equations, *Studies in Applied Mathematics*, 115(3), 2005, 303–318.
- [41] Kudenatti, R.B., Awati, V.B., Solution of pressure gradient stretching plate with suction, *Applied Mathematics and Computation*, 210(1), 2009, 151–157.
- [42] Rasheed, A., Anwar, M.S., Numerical computations of fractional nonlinear Hartmann flow with revised heat flux model, *Computers and Mathematics with Applications*, 76(10), 2018, 2421–2433.
- [43] Awati, V.B., Dirichlet series and approximate analytical method for the solution of MHD boundary layer flow of Casson fluid over a stretching/shrinking sheet, *TWMS Journal of Applied and Engineering Mathematics*, 7(2), 2017, 343–353.
- [44] Makinde, O.D., Awati, V.B., Bujurke, N.M., Dirichlet series and closed-form exact solutions of MHD Casson fluid flow over a permeable stretching/shrinking sheet, *Palestine Journal of Mathematics*, 10(1), 2021, 109–119.
- [45] Awati, V.B., Mahesh Kumar, N., Chavaraddi, K.B., Dirichlet series and approximate analytical solutions of MHD flow over a linearly stretching sheet, *International Journal of Industrial Mathematics*, 7(4), 2015, 343–350.
- [46] Puneeth, V., Ali, F., Khan, M.R., Anwar, M.S., Ahammad, N.A., Theoretical analysis of the thermal characteristics of Ree–Eyring nanofluid flowing past a stretching sheet due to bioconvection, *Biomass Conversion and Biorefinery*, 14(7), 2024, 8649–8660.
- [47] Awati, V.B., Dirichlet series and analytical solutions of MHD viscous flow with suction/blowing, *Applied Mathematics and Nonlinear Sciences*, 2(2), 2017, 341–350.
- [48] Alzahrani, J., Vaidya, H., Prasad, K.V., Rajashekhar, C., Mahendra, D.L., Tlili, I., Micro-polar fluid flow over a unique form of vertical stretching sheet: Special emphasis to temperature-dependent properties, *Case Studies in Thermal Engineering*, 34, 2022, 102037.
- [49] Hussain, Z., Muhammad, S., Anwar, M.S., Effects of first-order chemical reaction and melting heat on hybrid nanofluid flow over a nonlinear stretched curved surface with shape factors, *Advances in Mechanical Engineering*, 13(4), 2021, 1–12.
- [50] Anwar, M.S., Alam, M.M., Khan, M.A., Abouzied, A.S., Hussain, Z., Puneeth, V., Generalized viscoelastic flow with thermal radiations and chemical reactions, *Geoenergy Science and Engineering*, 232, 2024, 212442.
- [51] Lepik, Ü., Solving PDEs with the aid of two dimensional Haar wavelets, *Computers & Mathematics with Applications*, 61(7), 2011, 1873–1879.
- [52] Chen, C.F., Hsiao, C.H., Haar wavelet method for solving lumped and distributed parameter systems, *IEE Proceedings-Control Theory & Application*, 144, 1997, 87–94.
- [53] Hsiao, C.H., State analysis of the linear time delayed systems via Haar wavelets, *Mathematics and Computers in Simulation*, 44(5), 1997, 457–470.
- [54] Lepik, Ü., Numerical solution of evolution equations by the Haar wavelet method, *Applied Mathematics and Computation*, 185(1), 2007, 695–704.
- [55] Lepik, Ü., Solving fractional integral equations by the Haar wavelet method, *Applied Mathematics and Computation*, 214(2), 2009, 468–478.
- [56] Majak, J., Pohlak, M., Eerme, M., Application of the Haar wavelet-based discretization technique to problems of orthotropic plates and shells, *Mechanics of Composite Materials*, 45(6), 2009, 631–642.
- [57] Awati, V.B., Kumar, M., Wakif, A., Haar wavelet scrutinization of heat and mass transfer features during the convective boundary layer flow of a nanofluid moving over a nonlinearly stretching sheet, *Partial Differential Equations in Applied Mathematics*, 4, 2021, 100192.
- [58] Awati, V.B., Mahesh Kumar, N., Analysis of forced convection boundary layer flow and heat transfer past a semi-infinite static and moving flat plate using nanofluids-by Haar Wavelets, *Journal of Nanofluids*, 10(1), 2021, 106–117.
- [59] Merkin, J.H., On dual solutions occurring in mixed convection in a porous medium, *Journal of Engineering Mathematics*, 20(2), 1986, 171–179.
- [60] Harris, S.D., Ingham, D.B., Pop, I., Mixed convection boundary-layer flow near the stagnation point on a vertical surface in a porous medium: Brinkman model with slip, *Transport in Porous Media*, 77(2), 2009, 267–285.

ORCID iD

Vishwanath B. Awati  <https://orcid.org/0000-0002-2547-1058>

N. Mahesh Kumar  <https://orcid.org/0000-0003-3979-0452>

Akash Goravar  <https://orcid.org/0009-0001-2830-6402>





© 2024 Shahid Chamran University of Ahvaz, Ahvaz, Iran. This article is an open access article distributed under the terms and conditions of the Creative Commons Attribution-NonCommercial 4.0 International (CC BY-NC 4.0 license) (<http://creativecommons.org/licenses/by-nc/4.0/>).

How to cite this article: Awati V.B., Mahesh Kumar N., Goravar A. Stability Analysis of Mass Transfer on a Continuous Flat Plate Moving in Parallel or Reversely to a Free Stream in the Presence of Chemical Reaction by Haar Wavelets, *J. Appl. Comput. Mech.*, xx(x), 2024, 1–13. <https://doi.org/10.22055/jacm.2024.45656.4396>

Publisher's Note Shahid Chamran University of Ahvaz remains neutral with regard to jurisdictional claims in published maps and institutional affiliations.

